Journal of Nuclear Materials 381 (2008) 177–184

Contents lists available at ScienceDirect

Journal of Nuclear Materials

journal homepage: www.elsevier.com/locate/jnucmat

An innovative technique for evaluating fracture toughness of graphite materials

Jy-An John Wang *, Ken C. Liu

Oak Ridge National Laboratory, Oak Ridge, TN 37831-6069, United States

A B S T R A C T

Spiral notch torsion fracture toughness test (SNTT) was developed recently to measure the intrinsic fracture toughness (K_{IC}) of structural materials. The SNTT system operates by applying pure torsion to uniform cylindrical specimens with a notch line that spirals around the specimen at a 45° pitch. The K_{IC} values are obtained with the aid of a three-dimensional finite-element computer code, TOR3D-KIC. The SNTT method is uniquely suitable for testing a wide variety of materials used extensively in pressure vessel and piping structural components and weldments, including others such as ceramics, their composites, and concrete.

1. Introduction

The measure of fracture toughness is represented in terms of stress-intensity factor. The mode I (tensile opening mode) stress-intensity factor at the onset of rapid crack propagation under plane-strain conditions is defined as fracture toughness, K_{IC}, a controlling reference parameter used in design to avoid catastrophic brittle fracture. Adequate toughness is an essential attribute of structure systems design. American Society for Testing and Materials (ASTM) standard test methods, standard test method for plane-strain fracture toughness of metallic materials (E399) [1], are widely used to determine fracture toughness of metallic materials, using compact tension and compact disk tension specimens having thickness and volume sufficient to ensure the plane-strain condition at the crack front. Therefore, the accuracy and reliability of test results may be questionable if the specimen becomes excessively smaller than the minimum specimen size recommended by ASTM standard. Meeting the requirements is difficult and impractical because structure systems materials to be investigated may be geometrically unsuitable and/or have insufficient volume for making the standard specimen. Therefore, use of small specimens for K_{IC} measurement is essential for application to nuclear reactor pressure vessel safety surveillance because of the space limitation inside the reactor vessel. Clearly, there is a need of a new method to obtain valid data using small samples. In current engineering and regulatory practices, the fracture toughness safety margins set forth in nuclear reactor pressure vessels surveillance program are based on test results of Charpy V-notch (CVN) impact tests. The indirect method will inevitably yield results with elements of uncertainties; therefore, a large safety factor must be used to guard against unpredictabilities. If K_{IC} values can be directly determined without interpretation, the uncertainty and safety factor associated with current regulations on the safety assessment of material properties can be relaxed in a rational manner. Direct techniques to estimate in-service toughness degradation using a variety of pre-cracked specimens are under active development worldwide with emphasis on miniaturization.

Despite the international efforts on the development of small specimen testing techniques, no methods currently exist for direct measurement of K_{IC} for small specimens without a concern for size effect. Unlike the conventional test methods, the SNTT method is capable of testing small rod specimens that bear no resemblance to conventional compact tension specimens nor using conventional mode of loading. Therefore, the SNTT method is unique and innovative in both specimen design and loading concept.

Difficulties in testing of heat-affected zone (HAZ) and interpreting precarious test data have frustrated researchers to derive meaningful fracture toughness data [2–7]. The accurate determination of HAZ toughness will be immensely helpful to understand material degradation or recovery occurring in the course of service. Knowing chronological changes in HAZ toughness property will lead to effective control and improve HAZ material properties through proper processing and post-weld heat treatment. In welding processes, three zones of different material properties evolve, namely, base metal, weld metal, and HAZ. In the safety surveillance programs, the states of material degradation in all the three zones are considered to be equally important to structural integrity since they are inseparable. However, the HAZ is often evaluated differently from the other zones and even ignored from the integrity evaluation. This is due to the lack of an effective means to analyze the HAZ surveillance data, which often show inconsistent and severe data scatter attributed to metallurgical heterogeneity of the HAZ. Adequate test techniques to measure the K_{IC} of complex HAZ materials currently do not exist and are clearly needed.

* Corresponding author.
E-mail address: wangja@ornl.gov (J.-A.J. Wang).

0022-3115/$ - see front matter © 2008 Elsevier B.V. All rights reserved.
doi:10.1016/j.jnucmat.2008.07.034

Because the direction of crack growth is predictable, K_{IC} values can be reliably determined for functionally gradient materials and metal–matrix composites, using the SNTT method. Therefore, the SNTT method is a powerful technique for investigating the interfacial material properties at HAZ and functionally gradient materials.

In real structures fracture failure seldom occurs in a single mode, such as mode I in pure tension. Piping systems used in the chemical and petroleum industries cannot be constructed without curve-shaped components, such as elbows, U-bends and T-joints. While these components are effective in providing system flexibility to mitigate flexural loading (mode I loading), they also create torsional load (shear load known as mode III loading) to the piping system. Fracture behavior under mixed mode loading (modes I and III) is not well known partially due to the experimental difficulties with the test method using a CT specimen. The SNTT method has a significant advantage over the conventional methods to accomplish mixed mode fracture toughness testing by either using different pitch angle of the spiral groove or applying various combinations of loads in tension and torsion to the standard specimen.

2. Spiral notch torsion test (SNTT) system

A new method, spiral notch torsion test (SNTT) system (see Figs. 1 and 2), was developed for determining fracture toughness values for a wide spectrum of materials ranging from ductile to brittle materials. Limited test results obtained for steel, aluminum, graphite and mullite ceramic were compared and validated with those reported in the open literature [8–11]. The new method appears to be superior to existing test methods in terms of adherence to theory and experimental methodology. Although the general consensus has been supporting the method using compact-tension specimens as a standard method, some deficiencies in full compliance with the requirements of the classical theory of fracture mechanics remain. The SNTT test system operates by applying pure torsion to cylindrical specimens having a notch line that spirals around the specimen at a 45° pitch angle. The pure torsion creates a uniform equibiaxial tension/compression stress field on each of concentric cylinders and the grooved line effectively becomes a Mode I crack mouth opening. It is not difficult to visualize that the rod specimen is a different manifestation of a compact-tension specimen having a width equivalent to the total length of the spiral notch. Compact-tension specimen testing lacks a method to uniformly distribute applied load throughout the entire specimen thickness because the stresses at and near the two free surfaces are anomalous, resulting in shear lip formation often discernible in fractured specimens. In contrast, the torque load acting on every cross-section along the rod specimen is the same and directly measurable. A plane-strain condition is achieved on every plane normal to the spiral groove.

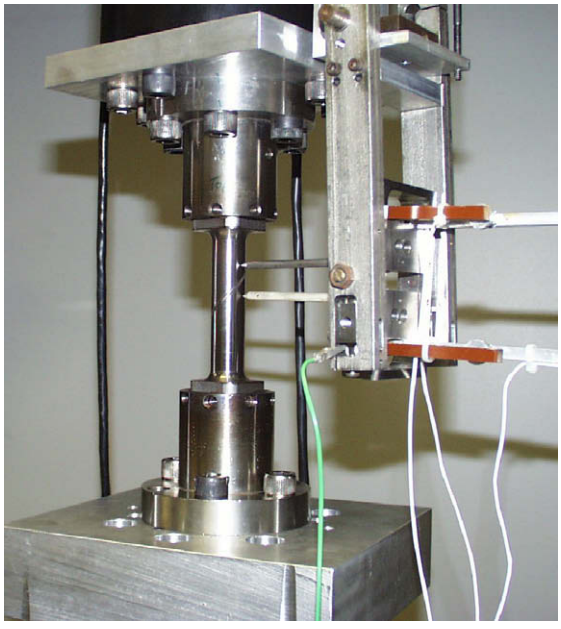

Fig. 1. SNTT test set-up.

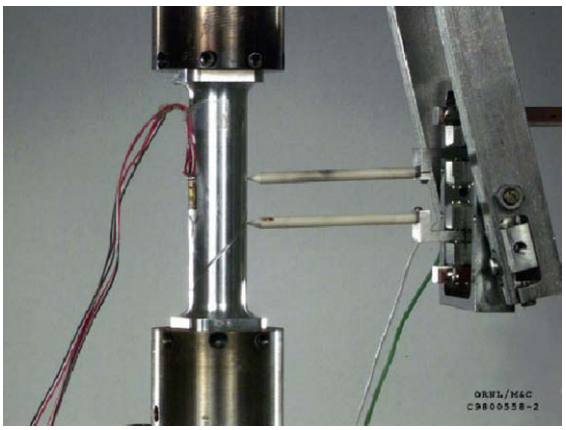

Fig. 2. Close view of SNTT set-up.

2.1. SNTT development goals

The motivations for developing the SNTT system are to:

- Generate intrinsic fracture toughness value.
- Eliminate specimen size effects.
- Establish a reliable and cost effective testing method.
- Generate consistent crack propagation.
- Minimize uncertainty in K_{IC} determination.
- Enable mixed-mode (Mode I + Mode III) fracture testing.

A series of feasibility study successfully demonstrated that the above six goals deficient in conventional testing methods have been achieved. After analytical evaluation of a 3-D non-coplanar crack front was completed, the fracture toughness was calculated using an in-house developed 3-D finite element code, TOR3D-KIC [12].

2.2. Basic theory of SNTT configuration

The SNTT test method uses a round rod specimen having a V-grooved spiral line with a 45° pitch (Fig. 3(a)), subjected to pure torsion. When the grooved specimen (Fig. 3(b)) is sectioned into segments perpendicular to the groove line, defined as *Z*-axis, each of the segments can be viewed as a CT specimen with a notch as illustrated in Fig. 3(c). Since all the imaginary CT specimens are bonded side-by-side seamlessly, the compatibility condition is automatically satisfied in every *XY*-plane, which remains in place before and after application of torsion loading.

In the absence of the V-groove, the stress state of a generic element in a round bar under pure torsion can be depicted as shown in Fig. 3(d), having the *XZ*-plane in tension and *XY*-plane in compression of equal magnitude. When a notch is introduced (Fig. 3(c)), the lateral sides of the wedge along the notch opening line will not contract because the stress in shaded area '*A*' is relieved. The disappearance of the tensile stress along the notch opening will shift the burden to the root of the notch, where a sharp rise will occur in the tensile σ_{yy} component. Since the un-

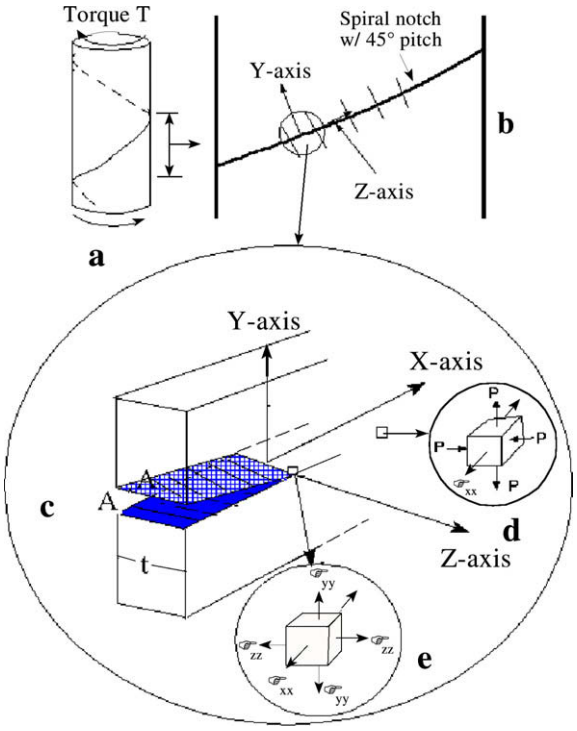

Fig. 3. Stress fields of a torsion bar.

stressed area 'A' does not contract in the *Z*-axis direction, while the material ahead of the notch root has a propensity to contract, a tensile stress field will develop in the σ_{zz} component in the root area of the notch. The transverse tensile stress σ_{xx} developing ahead of the notch front is due to the radial constraint. Therefore, a tri-axial tensile stress field will evolve in the neighborhood of the notch root area (see Fig. 3(e)). This observation has been experimentally and analytically validated from the feasibility study.

2.3. 3-D non-coplanar crack front

Due to the 3-D non-coplanar crack front of SNTT configuration and the lack of close form solutions, K_{IC} of SNTT method was evaluated using 3-D finite element analysis and derived from minimum strain energy density criterion [13]. The strain energy density criterion states that crack growth takes place in the direction of minimum strain energy density factor S. The 3-D energy density factor can be written [14] as

$$S = a_{11}K_{\mathrm{I}}^2 + 2a_{12}K_{\mathrm{I}}K_{\mathrm{II}} + a_{22}K_{\mathrm{II}}^2 + a_{33}K_{\mathrm{III}}^2,$$

where the stress intensity factors, K_{I}, K_{II}, and K_{III}, are evaluated from crack tip opening displacement (CTOD) of singular prismatic elements around the crack front (see Fig. 4, where CTODs are determined from a 3-D finite element analysis) and can be written as [15]

$$K_{\mathrm{I}} = \frac{E}{4(1-\nu^2)}\left(\sqrt{\frac{\pi}{2L_1}}\left[\begin{pmatrix} 2v_B - v_C + 2v_E - v_F + v_D \\ -2v_{B'} + v_{C'} - 2v_{E'} + v_{F'} - v_{D'} \end{pmatrix} + \frac{\eta}{2}\begin{pmatrix} -4v_B + v_C + 4v_E - v_F \\ +4v_{B'} - v_{C'} - 4v_{E'} + v_{F'} \end{pmatrix} + \frac{\eta^2}{2}\begin{pmatrix} v_{F'} + v_C - 2v_{D'} \\ -v_F - v_{C'} + 2v_{D'} \end{pmatrix}\right]\right),$$

$$K_{\mathrm{II}} = \frac{E}{4(1-\nu^2)}\left(\sqrt{\frac{\pi}{2L_1}}\left[\begin{pmatrix} 2u_B - u_C + 2u_E - u_F + u_D \\ -2u_{B'} + u_{C'} - 2u_{E'} + u_{F'} - u_{D'} \end{pmatrix} + \frac{\eta}{2}\begin{pmatrix} -4u_B + u_C + 4u_E - u_F \\ +4u_{B'} - u_{C'} - 4u_{E'} + u_{F'} \end{pmatrix} + \frac{\eta^2}{2}\begin{pmatrix} u_F + u_C - 2u_D \\ -u_{F'} - u_{C'} + 2u_{D'} \end{pmatrix}\right]\right),$$

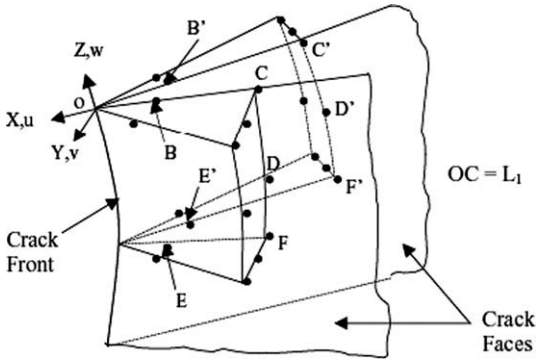

Fig. 4. Singular prismatic elements.

$$K_{\mathrm{III}} = \frac{E}{4(1+\nu)}\left(\sqrt{\frac{\pi}{2L_1}}\left[\begin{pmatrix} 2w_B - w_C + 2w_E - w_F + w_D \\ -2w_{B'} + w_{C'} - 2w_{E'} + w_{F'} - w_{D'} \end{pmatrix} + \frac{\eta}{2}\begin{pmatrix} -4w_B + w_C + 4w_E - w_F \\ +4w_{B'} - w_{C'} - 4w_{E'} + w_{F'} \end{pmatrix} + \frac{\eta^2}{2}\begin{pmatrix} w_F + w_C - 2w_D \\ -w_{F'} - w_{C'} + 2w_{D'} \end{pmatrix}\right]\right),$$

$$a_{11} = \frac{1}{16\mu}[(3 - 4\nu - \cos\theta)(1 + \cos\theta)],$$

$$a_{12} = \frac{1}{8\mu}[\sin\theta(\cos\theta - 1 + 2\nu)],$$

$$a_{22} = \frac{1}{16\mu}[4(1-\nu)(1-\cos\theta) + (3\cos\theta - 1)(1 + \cos\theta)],$$

$$a_{33} = \frac{1}{4\mu}.$$

where $\eta = 1$ at corner node, μ shear modulus, ν Poisson's ratio, and L_1 is singular element length.

The crack growth occurs when

$$S^* = S_{\mathrm{cr}} = \frac{1-2\nu}{4\mu}K_{\mathrm{IC}}^2.$$

Thus, K_{IC} can be estimated as

$$K_{\mathrm{IC}} = \sqrt{\left(\frac{4\mu}{1-2\nu}\right)(a_{11}K_{\mathrm{I}}^2 + 2a_{12}K_{\mathrm{I}}K_{\mathrm{II}} + a_{22}K_{\mathrm{II}}^2 + a_{33}K_{\mathrm{III}}^2)}, \quad \text{at} \quad \theta = \theta_0.$$

where θ_0 is the angle of crack extension.

In the SNTT configuration, the crack propagation orientation is directed toward and perpendicular to the axis of the cylinder, $\theta_0 = 0$. The other alternative to obtain K_{IC} is using *J*-integral approach based on domain integral method. Typically, a finite element model shown in Fig. 5(a) is used for brittle SNTT specimens with shallow crack front and Fig. 5(b) is for ductile specimens. The SNTT FEM model normally contains about 8000 20-node quadratic brick elements with reduced integration and 35,000 nodes.

2.4. FEM modeling

The TOR3D-KIC computer code was developed to simulate the 3-D spiral crack front and crack propagation orientation during transition phases between fatigue crack growth and the final fracture under pure torsion loading. TOR3D-KIC is used as a means to calculate mode-I fracture toughness of solid materials, using a round rod-specimen having a prefabricated spiral V-grooved line with a 45° pitch on the specimen surface. Mixed mode fracture toughness values in various combinations of mode I, II, and III, are derived with different spiral pitchs.

TOR3D-KIC uses three-dimensional finite element techniques to analyze the crack tip opening displacement (CTOD) occurring on a

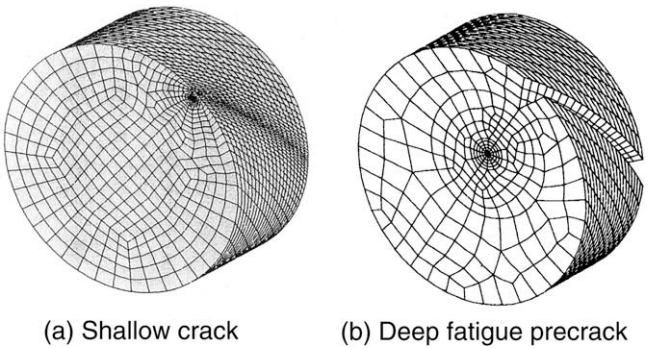

Fig. 5. SNTT FEM models.

non-coplanar 3-D spiral crack front. An iterative process is used to update the boundary conditions of the finite element method (FEM) and match the fracture load with imposed torsion load. 3-D wedge singular elements adjacent to the crack front are used to simulate the $r^{-1/2}$ stress singularity at the crack tip. Based on the input of the fracture load and final crack length, the CTODs at the crack flange along the crack front are analyzed and then integrated into a mode I fracture toughness formulation using minimum strain energy criteria.

2.5. SNTT specimen size reduction

The CT specimen, as shown in the upper area of Fig. 6, has been widely used in existing fracture toughness test methods because the general consensus indicates it is the next-best basic configuration that nearly conforms to the strict requirements of the classical theory of fracture mechanics. Despite the simplification, the theoretical conditions (i.e., the conditions required to achieve uniformly distributed applied stress over the thickness and plane-strain condition) can never materialize as long as the free surfaces exist at both ends. The end effects will be further amplified when the thickness decreases to a thin plate, as shown in Fig. 6. Another dilemma is that an increase in specimen thickness will automatically accompany an increase in specimen length and width in order to maintain specimen rigidity under load.

To circumvent those problems, the SNTT System was developed and predictions were evaluated for comparison with published data to validate the method. In conforming to the stress and strain constraints, which are conditions necessary to validate the use of fracture mechanics theory, a round rod specimen is subjected to pure torsion, as shown in Fig. 7. The pure torsion generates an equibiaxial tension/compression stress field on ±45°-pitched orthogonal planes along the right conoids (radii emanating from the center axis at a 90° angle), independent of the specimen diameter. A plane-strain condition is maintained on every plane normal to the spiral groove.

Because of the plane strain and axisymmetric constraint and the uniformity in the stress and strain fields, the crack front must propagate perpendicularly toward the specimen axis along the conoids. Post-mortem examination verified the crack propagation behavior (see Fig. 8). When a lobe of V-grooved spiral line with a 45° pitch is machined on the surface of the specimen, the grooved line effectively becomes a Mode I crack mouth opening. Examination reveals that the rod specimen is a different manifestation of a CT specimen having a thickness equivalent to the full length of the spiral line (Fig. 9). It should be noted that the round specimen with a helical notch also suffers the end effect at the notch line ends as discussed earlier in the case of the CT specimen. However, with the aid of Fig. 9, it is not difficult to illustrate that the load distribution along the notch line on the round specimen is statically determinable in nature whereas the situation in the CT specimen is a statically indeterminate problem.

For the sake of discussion, the thick CT specimen is assumed to be sectioned vertically in a number of equal segments, and the round rod specimen is also cross-sectioned in a number of discs having equal thickness, as shown in Fig. 9. Because the end segments in the CT specimen are anomalies that have a free surface, the applied tensile load cannot be distributed evenly to all the segments. A statically indeterminate problem as discussed above is theoretically somewhat complex but manageable, whereas it is experimentally hopeless, if not impossible, to solve the problem. When the rod specimen is subjected to pure torsion, all the discs are subjected to the same torque load and the exact amount of the torque load is known. It is a statically determinate problem.

Miniaturization is an important goal. This is made possible because the K_{IC} values determined by the SNTT method are virtually independent of specimen size. A cursory review of the stress and strain fields in a CT specimen indicates that the key information needed for determining the K_{IC} values is manifested within a small region near the crack tip; therefore, the rod specimen can be miniaturized substantially without the loss of general validity (Fig. 6). The purpose of the vast volume of the material outside the critical

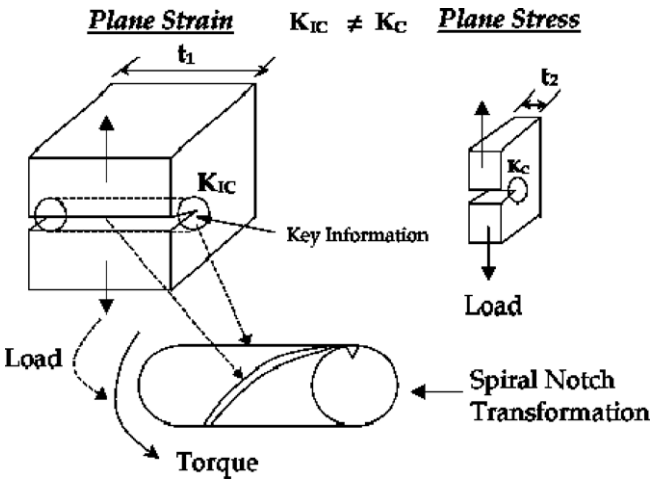

Fig. 6. Specimen size effect.

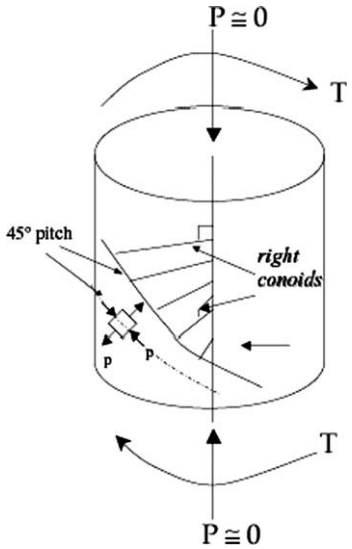

Fig. 7. Pure torsion.

Fig. 8. 7475-T7351 aluminum.

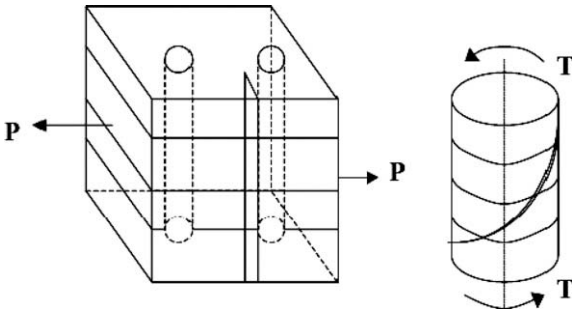

Fig. 9. Applied load distribution.

zone in conventional samples is to poise the ideal far field of stress and to provide a means to accommodate loading devices. This redundancy is eliminated to the optimum condition in the round rod specimen; therefore, the specimen miniaturization is achievable.

2.6. Mixed-mode fracture toughness

In a recent study of mixed-mode fracture [16], utilizing a complex test set-up with a specially machined CT specimen, test results indicate that mixed-mode (Mode I + Mode III) toughness and tearing modulus reduced to 50% and 30%, respectively, compared to those under Mode I only for some ductile materials. Therefore, the synergistic impact due to the combination of flexural normal stress (Mode I fracture) and the torsion shear stress (Mode III fracture) to the fracture toughness of the materials used in pressure vessel and piping (PVP) systems may need a review.

3. Experimental procedures and results

Torsion tests were performed on a closed-loop controlled, electro-hydraulic, biaxial testing system shown in Fig. 1. Shear strain was measured using a biaxial strain extensometer and a Rosette strain gage (shown in Fig. 2) for cross calibration. Pure torsion was achieved with a zero axial force in control. Pre-cracking for metallic specimens was accomplished with cyclic torsion using Haver sine wave form. The maximum torque used in pre-cracking varies with materials and must be determined experimentally. In the case of an A302B steel sample with 0.075 in. notch, 60–80% of the torque that generates the shear stress of 300 MPa around the specimen diameter will suffice, yielding a ΔK in the range of 20–25 MPa$\sqrt{m}$. The fatigue crack growth was measured by post-mortem examination.

Fig. 10 shows the geometry of the specimen used in K_{IC} measurements of metallic alloys. The specimen has a uniform gage section on which a complete lobe of spiral V-groove with a pitch of 45° is shown for mode I testing. The pitch angle can be tailored for a mixed mode test. The squared end sections were made to transmit torque and the threaded ends for zero axial load control. The size of the test specimen is optional depending on the availability of the material. Specimens were fabricated from a 2-in. thick plate of 7475-T7351 aluminum alloy and a block of A302B steel. Observation of the fracture surface of 7475-T7351 aluminum specimen indicates that crack propagation orientation is toward and perpendicular to the central axis of torsion specimen. The reader is referred to Ref. [9] for experimental details and test results of metallic materials.

3.1. Ceramic material testing

Ceramic materials are usually available in a small volume, and small round rods are most common. Mullite ceramic material was selected in this experiment. A straight mullite ceramic rod, having each end bonded with epoxy adhesive to a square-ended metal holder of the same design used in the metal specimens, was used in the experiment. Fatigue precracking can be waived for K_{IC} evaluation by using SNTT on brittle materials. For the test

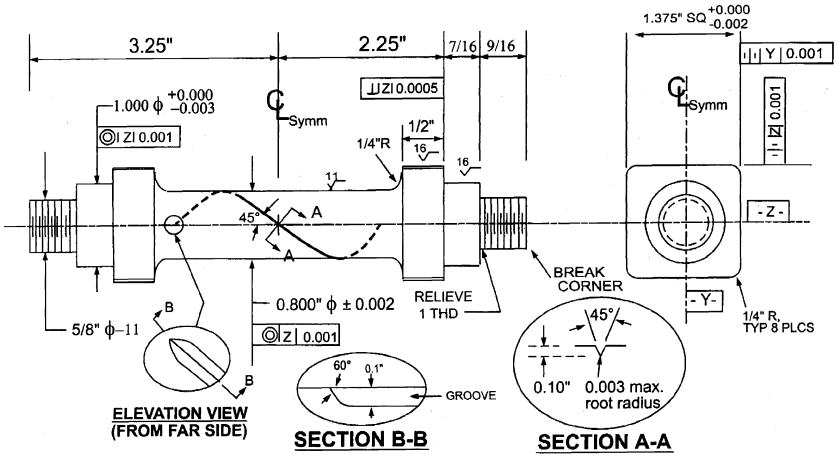

Fig. 10. SNTT specimen configuration.

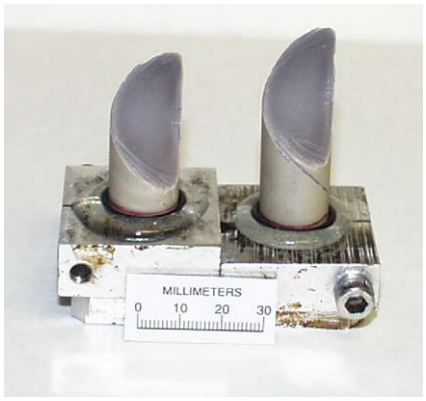

Fig. 11. SNTT mullite sample.

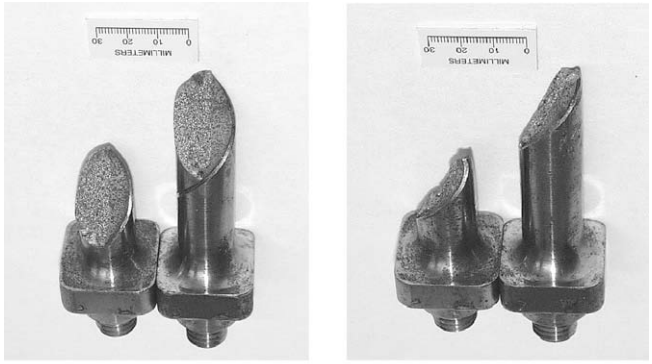

Fig. 12. The SNTT A302B specimen.

on mullite ceramic, a shallow spiral V-groove with a depth of 0.5-mm on the uniform gage section of 17-mm diameter was sufficient. The specimen failed at 49.67 N m torque at room temperature. Postmortem examination indicates that the failure mode is a brittle fracture along the helix (Fig. 11). The K_{IC} was estimated as 2.21 MPa$\sqrt{}$m obtained by SNTT and reported as 2.20 MPa$\sqrt{}$m in ORNL report [17].

3.2. A302B steel testing

The A302B specimen (Fig. 12) has a uniform gage section of 20.3-mm diameter and 76.2-mm gauge length. A A302B specimen having a spiral V-groove with a depth of 1.9-mm was tested. An exploratory fatigue precrack procedure was used to control crack growth with reference to the change in slope of the load–displacement curves. The specimen (Fig. 12) fractured at 519.7 N m torque at room temperature. Test results obtained from the strain gage and biaxial extensometer are shown in Fig. 13(a) and (b), respectively. Postmortem examination indicates that the final failure mode is brittle fracture.

A recent effort on developing fatigue precrack protocol for using miniature SNTT samples of A533B steel was successful. A comparison of fractures obtained from the prototype and miniature test specimens is illustrated in Fig. 14.

3.3. MA956 inconel alloy

Because of limited availability of alloy MA956, four small SNTT samples with diameter of 3.8 mm (0.15 in.) were used for exploring fatigue precrack and fracture behavior for the as-received (non-oxidized) alloy. Three SNTT MA956 specimens were used for evaluating the fatigue precrack procedures. This fatigue precrack procedure was then used to precrack some of the SNTT baseline samples. The sample of MA956 was fractured at 32 N-m with a 0.06-in. deep crack. The estimated toughness of the as-received MA956 material was about 68 MPa$\sqrt{}$m. The fracture SNTT samples are shown in Fig. 15.

3.4. Graphite material

A pilot study of applying SNTT to graphite material was also carried out. A shallow spiral groove was machined on the SNTT sample, no further precrack was provided to the SNTT graphite samples. The estimated fracture toughness of SNTT graphite samples is 1.0 MPa$\sqrt{}$m, and the fracture SNTT samples of 15-mm and 25.4-mm diameter are shown in Figs. 16 and 17, respectively.

3.5. Fracture toughness evaluation

A summary of K_{IC} value for A302B steel, 7475-T7351 aluminum, mullite ceramic, MA956 alloy, and graphite are stated in Table 1.

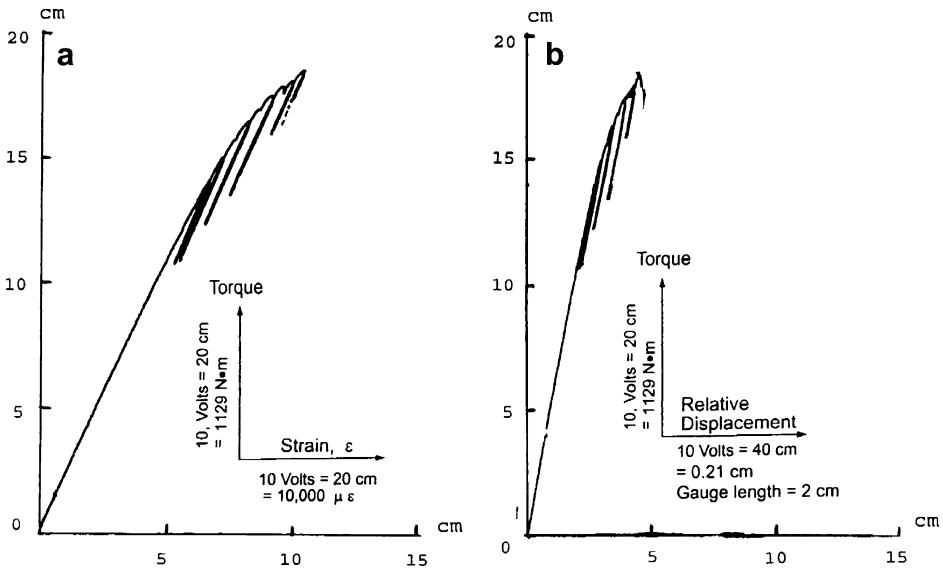

Fig. 13. Plot of torsion test results from (a) load cell and strain gauge, and (b) load cell and biaxial extensometer.

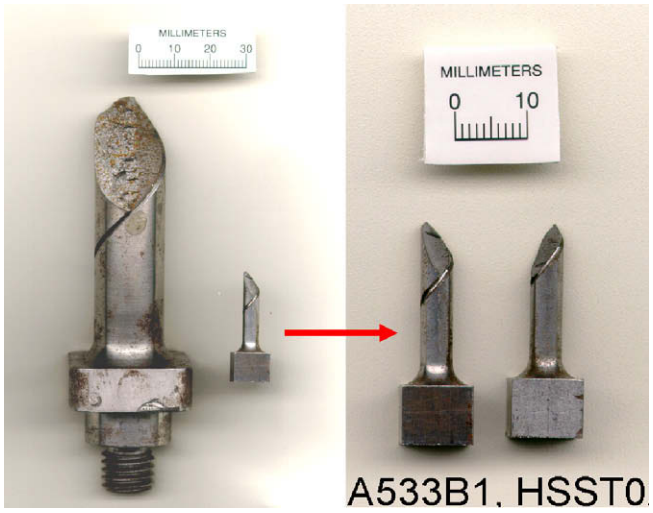

Fig. 14. SNTT specimen miniaturization.

The reader is referred to Ref. [9,10] for details of fracture toughness evaluations (see Figs. 18).

Due to the limited experimental data obtained, no uncertainty analysis was carried out. However, the long crack front and the stringent plane strain condition should yield less uncertainty compared to conventional test methods. The characteristic features of the uniform crack fronts discerned in tested torsion samples appear to support the above statement.

4. Conclusions

A new torsion bar testing method, SNTT, has been developed for estimating the opening mode fracture toughness, K_{IC}. A round-bar specimen having a spiral V-groove line at 45° pitch is used, subjected to pure torsion. Commercially available mullite ceramic, graphite, MA956 Inconel, 7475-T7351 aluminum, and A302B steel were tested. The K_{IC} values for the materials were estimated with the aid of a 3-D FEA code (TOR3D-KIC) based on the fracture load and final crack length data. Predicted values derived from SNTT were compared with ORNL CT data, those reported by vendors, and those available in the open literature. Results show that K_{IC} values estimated from SNTT are nominally higher than those from vendor's data by 0.2% for mullite material, 0.8% for 7475-T7351 aluminum, and 1.6% for A302B steel. The vendor's CT data in the TL orientation (crack propagate in the rolling direction) [1] is comparable to the torsion data. Agreement between the SNTT data and

Fig. 15. Fractured MA956 SNTT samples.

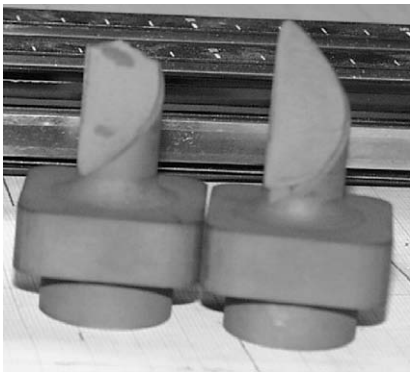

Fig. 16. Fractured graphite SNTT samples, 15-mm dia.

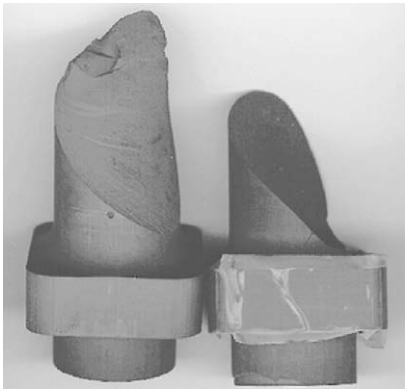

Fig. 17. Fractured graphite SNTT samples, 25-mm dia.

Table 1
SNTT K_{IC} evaluation

Materials	K_{IC} (MPa$\sqrt{m}$)	
	SNTT	Method conventional[a]
A302B steel	55.8	55.0 CT
7475-T7351 Al	51.3	51.0 Vendor/CT
Mullite ceramic	2.21	2.20 3P
MA956 Inconel	68	Not available
Graphite	1.0	1.0 Vendor/CT

[a] In TL orientation and at room temperature.

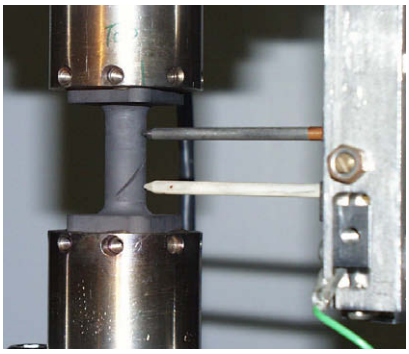

Fig. 18. SNTT graphite test set-up.

data reported in the literature is remarkable, in view of possible material variation, inhomogeneity, and anisotropy, indicating the proposed method is a reliable technique.

The unique features of the proposed testing method are:

- It conforms to the classical theory of fracture mechanics.
- It is not limited by sample size or volume.
- It can test multiple modes of stress (e.g., flexural normal stress and torsional shear stress) simultaneously.
- It controls crack propagation and thus produces consistent results.
- It can test a wide variety of materials, such as metals and alloys (including the heat-affected zone of welds), ceramics, composites, polymers, carbon foam, and concrete.
- It does not require fatigue precracking of brittle samples.
- It has a potential for use to determine the K_{IC} values of interface of inhomogeneous material [18] and mechanical properties of HAZ.

The SNTT technique is envisaged to offer new opportunities for use in material research, particularly in the field of welding technology, and as an effective and economical tool for nuclear PVP system surveillance use.

Acknowledgements

The research was sponsored by the ORNL LDRD Program, and Heavy Vehicle Propulsion System Materials Program, DOE Office of Heavy Vehicle, under contract DE-AC05-00OR22725 with UT-Battelle, LLC.

References

[1] ASTM Test Method for Plane-Strain Fracture Toughness of Metallic Materials (E399).
[2] H.S. Chung, T. Takahashi, M. Suzuki, Weld. World 16 (1978) 248.
[3] J.Y. Koo, A. Ozekcin, A Local Brittle Zone Microstructure and Toughness in Structure Steel Weldments, in: J.Y. Koo (Ed.), Proceedings of an International Symposium on Welding Metallurgy of Structural Steels, Denver, Colorado, 1987.
[4] C.D. Lundin, Weld. Res. Bull. 295 (1986).
[5] R.E. Dolby, G.L. Archer, in: Proceedings of the Practical Applications of Fracture Mechanics to Pressure Vessel Technology Conference, 1971.
[6] D.O. Hobson, R.K. Nanstad, Effects of Off-Specification Procedures on the Mechanical Properties of Half-Bead Weld Repairs, Oak Ridge National Laboratory Report NUREG/CR-3265,ORNL/TM-8661, 1983.
[7] J.P. Tronskar, J. Offshore Mech. Arctic Eng. 117 (1995) 46.
[8] J.A. Wang, K.C. Liu, D.E. McCabe, S.A. David, An Innovative Small Specimen Testing Technique for the Determination of Fracture Toughness, Oak Ridge National Laboratory Report, ORNL/M-6366, 1999.
[9] J.A. Wang, K.C. Liu, D.E. McCabe, S.A. David, J. Fatigue Fract. Eng. Mater. Struct. 23 (2000) 45.
[10] J.A. Wang, K.C. Liu, D.E. McCabe, in: W.G. Reuter, R.S. Piascik, (Eds.), Fatigue and Fracture Mechanics, vol. 33, December 2002, ASTM STP 1417, p. 757.
[11] J.A. Wang, K.C. Liu, and G.A. Joshi, in: ASME Proceeding of ETCE 2002 Conference on Composite Materials Design & Analysis, 3–4 February 2002, Houston, Texas.
[12] J.A. Wang, TOR3D-KIC: A 3-D Finite Element Analysis Code for Determination of Fracture Toughness, K_{Ic}, for Spiral Notch Torsion Fracture Test (SNTT), Oak Ridger National Laboratory report ORNL LTR Report, 2001.
[13] G.C. Sih, Int. J. Fract. 10 (1974) 305.
[14] R.J. Hartranft, G.C. Sih, Eng. Fract. Mech. 9 (1977) 705.
[15] R.S. Barsoum, Int. J. Numer. Meth. Eng. 11 (1977) 85.
[16] H.-X. Li, R.H. Jones, J.P. Hirth, D.S. Gelles, J. Nucl. Mater. 233 (1998) 258.
[17] W.J. Lackey, D.P. Stinton, G.A. Cerny, L.L. Fehrenbacher, A.C. Schaffhauser, Ceramic Coating for Heat Engine Materials – Status and Future Needs, Oak Ridge National Laboratory report, ORNL/TM-8959, Oak Ridge National Laboratory.
[18] Jy-An John Wang, Ian G. Wright, Michael J. Lance, Ken C. Liu, Mater. Sci. Eng. A 426 (2006) 332.